Article

JOURNAL OF THE CHINESE CHEMICAL SOCIETY

β-$AgVO_3$ Nanorods as Peroxidase Mimetic for Colorimetric Determination of Glucose

Junyu Lu, Lianqiang Wei, Dongmei Yao, Xiuju Yin, Hongfang Lai* and Xiuxiang Huang*

College of Chemistry and Biology Engineering, Hechi University, Yizhou 546300, China

(Received: January 22, 2017; Accepted: April 5, 2017; DOI: 10.1002/jccs.201700031)

β-$AgVO_3$ nanorods have been demonstrated to exhibit intrinsic peroxidase-like activity. The oxidation of glucose can be catalyzed by glucose oxidase (GO*x*) to generate H_2O_2 in the presence of O_2. The β-$AgVO_3$ nanorods can catalytically oxidize peroxidase substrates including *o*-phenylenediamine (OPD), 3,3′,5,5′-tetramethylbenzidine (TMB), and diammonium 2,2′-azino-bis (3-ethylbenzothiazoline-6-sulfonate) (ABTS) by H_2O_2 to produce typical color reactions: OPD from colorless to orange, TMB from colorless to blue, and ABTS from colorless to green. The catalyzed reaction by the β-$AgVO_3$ nanorods was found to follow the characteristic Michaelis–Menten kinetics. Compared with horseradish peroxidase and $AgVO_3$ nanobelts, β-$AgVO_3$ nanorods showed a higher affinity for TMB with a lower Michaelis–Menten constant (K_m) value (0.04118 mM) at the optimal condition. Taking advantage of their high catalytic activity, the as-synthesized β-$AgVO_3$ nanorods were utilized to develop a colorimetric sensor for the determination of glucose. The linear range for glucose was 1.25–60 μM with the lower detection limit of 0.5 μM. The simple and sensitive GO*x*-β–$AgVO_3$ nanorods–TMB sensing system shows great promise for applications in the pharmaceutical, clinical, and biosensor detection of glucose.

Keywords: β-$AgVO_3$ nanorods; Peroxidase-like activity; Colorimetric assays; Glucose detection.

INTRODUCTION

Because of its low cost, simplicity, and fast detection, colorimetric sensing is considered a very important method in analytical chemistry. Significantly, it can be employed during field analysis using only naked eyes. Colorimetric sensing does not demand any expensive or complicated instrumentation because the changes of color can be directly visualized.[1] However, this analytical method also faces some challenges, including how to turn the detection events into obvious color changes.[2] Today, peroxidase working as colorimetric sensing agent has been extensively approved in many fields. It can catalytically oxidize substrates including *o*-phenylenediamine (OPD), 3,3′,5,5′-tetramethylbenzidine (TMB), and diammonium 2,2′-azino-bis(3-ethylbenzothiazoline-6-sulfonate) (ABTS) to generate color changes.[3] Unfortunately, the natural enzyme suffers from some intrinsic disadvantages, for example, lack of stability, tedious preparation and purification processes, and inactivity under harsh conditions. In order to overcome these shortcomings, many efforts have been made to develop peroxidase mimetics.[4]

In recent years, a number of nanomaterials have emerged owing to the widespread development of nanoscience and technology. They have been widely applied in various fields because of their intrinsic advantages such as low cost, easy preparation and purification, good stability, and stable storage. Some of nanomaterials have shown potential for colorimetric sensing.[5] Hupp *et al.*[6] used an Au-nanoparticle-based colorimetric sensor for the determination of heavy metal ions. However, the change of color based on Au nanoparticles was dependent on their size, capping agents, and shape.[7] These drawbacks limit their application. To overcome these shortcomings, many attempts have been made to develop peroxides mimetics. Since Yan' group[8] showed that inorganic materials of Fe_3O_4 magnetic nanoparticles possess intrinsic peroxidase-like activity, a number of the inorganic materials were found to possess enzyme-like activity. Such materials include metallic oxide nanoparticles (CeO_2,[9] Co_3O_4,[10] V_2O_5,[11] CuO,[12] and MnO_2,[13]), metallic and bimetallic nanostructures (Au,[14] Ag,[15] Pt,[16] AFt-Fe-Pt,[17]and Au@PtAg[18]), carbon-based

*Corresponding authors. Email: laihongfang263@163.com; hxx1372@sina.com

nanomaterials (graphene oxide,[19] carbon nanotubes,[20] carbon dots[21]), and bimetallic oxide nanoparticles ($ZnFe_2O_4$,[22] $CoFe_2O_4$,[23] $FeWO_4$,[24] and $NiFe_2O_4$[25]), which have been applied in colorimetric sensing based on their peroxides-like activity. Among them, the bimetallic oxide alum was not included until Zhang *et al.*[26] reported that $AgVO_3$ nanobelts exhibited intrinsic peroxidase-like activity. However, $AgVO_3$ nanobelts had a large size, which affected its catalytic activity. Yan *et al.*[8] found that the smaller the size of a nanozyme, the higher its catalytic activity due to the larger surface area for interaction with substrates. Therefore, developing smaller alum bimetallic oxides with peroxidase-like activity still remains a challenge.

In this work, a simple and easy hydrothermal method was used for the preparation of small β-$AgVO_3$ nanorods. The catalytic activity of these nanorods was investigated by the catalytic oxidation of TMB to produce a typical blue color reaction in the presence of H_2O_2. Glucose oxidase (GO*x*) could catalyze the oxidation of glucose to generate H_2O_2 (Scheme 1). Based on these findings, a simple and quick colorimetric method was developed to determine glucose in serum samples.

EXPERIMENTAL

Chemicals and materials

All chemicals in this work were obtained from commercial sources and used as received without further purification. Unless otherwise stated, all the chemicals were analytical grade. Acetic acid (HAc), calcium chloride ($CaCl_2$), potassium carbonate (K_2CO_3), H_2O_2 (30 wt %), and sodium acetate (NaAc) were obtained from Shantou Xilong Chemical Factory (Guangdong, China). TMB, ABTS, and OPD were purchased from TCI (Shanghai, China). Silver nitrate ($AgNO_3$), partial ammonium vanadate (NH_4VO_3), glucose, lactose, fructose, ascorbic acid (AA), and *tert*-butyl alcohol were purchased from Aladdin Chemistry Co. Ltd (Shanghai, China). GO*x*, horse radish peroxidase (HRP), and glutathione (GSH) were obtained from Sigma-Aldrich (St. Louis, MO, USA). Ultrapure water was produced by a Millipore purification system (Bedford, MA, USA) and used to prepare all aqueous solutions. Human serum samples were obtained from the Five People's Hospital of Guilin (Guilin, China). All experiments were performed in compliance with the relevant laws and institutional guidelines of the ethics committee of the hospital, and informed consent was obtained from the patients who provided the human samples.

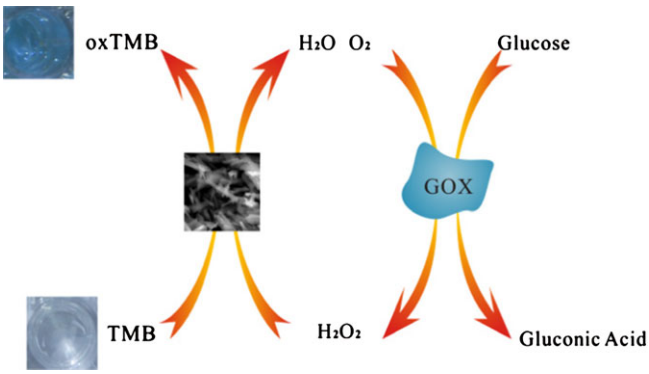

Scheme 1. Schematic illustration of colorimetric determination of glucose using GO*x*–β-$AgVO_3$ nanorod-catalyzed reactions.

Apparatus

Absorption spectra were obtained on a Cary 60 model spectrophotometer (Agilent, Santa Clara, CA, USA). The powder X-ray diffraction (XRD) patterns of β-$AgVO_3$ were recorded on a D/max 2550 VB/PC diffractometer (Rigaku,Tokyo, Japan) with Cu Kα radiation (λ = 0.15418 nm). Scanning electron microscopy (SEM) was carried out on an FEI Quanta 200 FEG SEM instrument (Philips, Amsterdam, Netherlands). Inductively coupled plasma mass spectrometry (ICP-MS) was carried out on a Flexar/NexlON300X apparatus (PerkinElmer, Waltham, MA, USA).

Synthesis of β-$AgVO_3$ nanorods

The β-$AgVO_3$ nanorods were prepared according to the literature[27] with some modification. Typically, 0.170 g of $AgNO_3$ was added to 30 mL ultrapure water with magnetic stirring. Then, 0.085 g of NH_4VO_3 was added to this solution. The mixed solution was continuously stirred for 2 h. The solution was transferred to a Teflon-lined stainless steel autoclave and heated for 24 h at 180°C. After cooling to room temperature, the yellow product was isolated by centrifugation and was washed several times with ultrapure water and ethanol in order to remove the superfluous reactants. Finally, the β-$AgVO_3$ nanorods were dried in a vacuum oven for 6 h at 60°C.

Mimetic peroxidase activity assays

All the reactions were monitored in the time-scan mode at 652 nm using the Cary 60 spectrophotometer. Kinetic measurements were carried out by monitoring the absorbance change at 652 nm. A typical catalytic experiment was as follows: 4.5 μg/mL β-$AgVO_3$ nanorods or 0.3 ng/mL HRP, 0.1 mM TMB, and 8 mM H_2O_2 were taken as the substrates in a reaction volume of 2 mL. The kinetic constants were calculated by employing the Lineweaver–Burk plots of the double reciprocal of the Michaelis–Menten equation: $1/\nu = V_{max} \times [S]/(K_m + [S])$, where the ν is the initial velocity, V_{max} is the maximum reaction velocity, [S] is the concentration of the substrate, and K_m is the Michaelis constant[8].

Colorimetric detection of glucose

Colorimetric detection of glucose was carried out as follows: (a) 50 μL of GO*x* (1 mg/mL) and 50 μL of glucose at various concentrations in phosphate buffered saline (PBS) (10 mM, pH 6.9) were incubated at 37°C for 30 min; (b) 25 μL of TMB (4 mM), 90 μL of β-$AgVO_3$ nanorods (0.05 mg/mL), and 585 μL of 0.2 M NaAc–HAc buffer (pH 4.0) were successively added into the above 300 μL glucose reaction solution; (c) the mixed solution was incubated at room temperature for 25 min; and (d) the absorption spectrum of mixed solution was determined by the spectrophotometer.

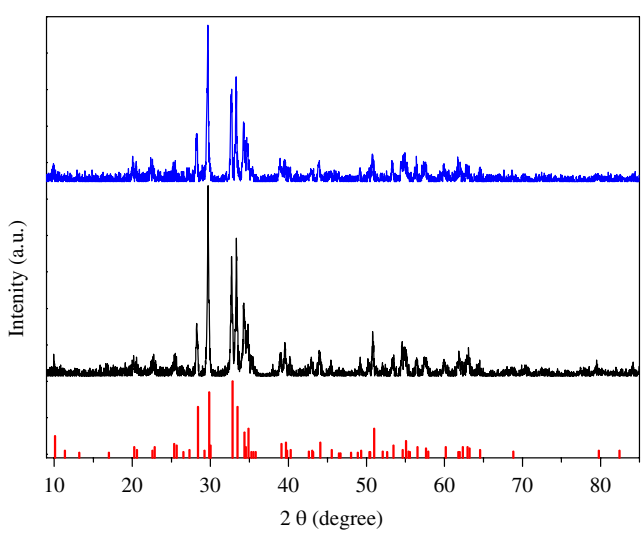

Fig. 1. XRD pattern of the β-$AgVO_3$ nanorods before (black line) and after a catalytic reaction (blue line).

For glucose detection in real samples, the human serum samples were diluted 20-fold with ultrapure water. A certain amount of the diluted solution was added to 10 mM PBS (pH 6.9) and 50 μL of GO*x* (1 mg/mL), and various concentrations of the glucose solutions were spiked. The mixed solution was dealt with in the same way as the glucose standard. The mixed solutions were analyzed with the proposed method, and the percent recovery values were obtained. In the selectivity experiments, 600 μM AA, 600 μM fructose, 600 μM K_2CO_3, 600 μM $CaCl_2$, 600 μM lactose, and 600 μM glutathione were used to replace 60 μM glucose.

RESULTS AND DISCUSSION

Characterization of β-$AgVO_3$ nanorods

The β-$AgVO_3$ nanorods were synthesized by a hydrothermal method. The morphology and structure of the as-synthesized β-$AgVO_3$ nanorods were identified by XRD, SEM, and ICP-MS. Figure 1 shows the XRD patterns of as-synthesized β-$AgVO_3$ nanorods before and after the catalytic reaction. The diffraction peak positions coincided with those of the standard cards (JCPDS 29–1154), which indicated that the prepared β-$AgVO_3$ nanorods had a well-crystallized structure. At the same time, it also demonstrated that the as-synthesized β-$AgVO_3$ nanorods had good stability in this sensing system. The SEM images showed that the prepared β-$AgVO_3$ exhibit nanorod-like morphology. The nanorod diameter was 28–80 nm and the length was 0.4–1.2 μm (Figure 2). The obtained β-$AgVO_3$ nanorods were smaller than the $AgVO_3$ nanobelts,[26] which indicated that the catalytic activity of β-$AgVO_3$ nanorods should be higher than that of the $AgVO_3$ nanobelts. The as-prepared sample was investigated using ICP-MS (Table 1). This analysis indicated that the compositions of Ag and V were close to the theoretically calculated values, suggesting that β-$AgVO_3$ nanorods were successfully synthesized.

Peroxidase-like activity of β-$AgVO_3$ nanorods

The β-$AgVO_3$ nanorods are a kind of inorganic material with expected enzyme-like activity. The peroxidase-like activity of β-$AgVO_3$ nanorods was studied by the catalytic oxidation a typical peroxidase substrate (TMB) via H_2O_2. As shown in Figure 3(a), β-$AgVO_3$ nanorods, TMB + β-$AgVO_3$ nanorods,

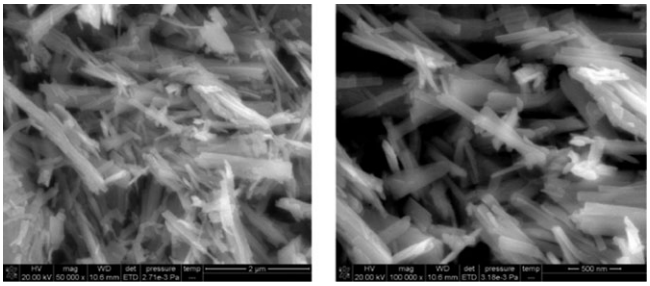

Fig. 2. SEM images of the as-prepared β-$AgVO_3$ nanorods.

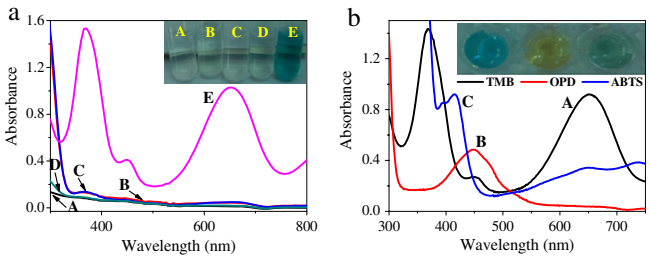

Fig. 3. (a) UV–vis spectra of (A) β-$AgVO_3$ nanorod solution, (B) TMB + β-$AgVO_3$ nanorods, (C) TMB–H_2O_2, (D) H_2O_2 + β-$AgVO_3$ nanorods, and (E) TMB–H_2O_2–β-$AgVO_3$ nanorod solution at pH 4.0 HAc–NaAc buffer at 25°C. ([TMB]: 0.1 mM, [H_2O_2]: 8 mM, [β-$AgVO_3$]: 4.5 μg/mL). (b) The β-$AgVO_3$ naonorod-catalyzed oxidation of diverse substrates to produce various color reactions. (A) TMB, (B) OPD, (C) ABTS. Inset: (a) photographs of aqueous solution of β-$AgVO_3$ nanorods (A), TMB + β-$AgVO_3$ nanorods (B), TMB–H_2O_2 (C), H_2O_2 + β-$AgVO_3$ nanorods (D), and TMB–H_2O_2–β-$AgVO_3$ nanorods (E). (b) The corresponding photograph of these samples.

TMB–H_2O_2, or H_2O_2+β-$AgVO_3$ nanorod system did not produce a typical blue color reaction. However, the TMB–H_2O_2–β-$AgVO_3$ nanorod system could produce a color reaction. Meanwhile, two remarkable absorbance peaks could be observed at 370 and 652 nm, which were caused by the oxidation product of TMB. In order to demonstrate the peroxidase-like catalytic ability of β-$AgVO_3$ nanorods further, two other typical peroxidase substrates (OPD, ABTS) were also studied (Figure 3(b)). These results showed that β-$AgVO_3$ nanorods exhibited an intrinsic peroxidase-like catalytic activity and could catalyze the oxidation of TMB in the presence of H_2O_2.

The absorbance changes of oxidized TMB at 652 nm depend on the concentration of β-$AgVO_3$ nanorods and reaction time (Figure 4). The absorbance gradually increased with increasing β-$AgVO_3$ nanorod concentration, which further confirmed that β-$AgVO_3$ nanorods exhibited peroxidase-like ability for the catalytic oxidation of TMB to produce a typical color reaction. In order to prove the catalytic mechanism of β-$AgVO_3$ nanorods, *tert*-butyl alcohol was applied as a typical $^{\cdot}OH$ radical capture reagent in the β-$AgVO_3$ nanorods+TMB+ H_2O_2 reaction system (Figure 5). *tert*-Butyl alcohol could rapidly react with OH and terminate radical chain reactions by generating inert intermediate radicals.[28] The experimental results showed that the absorbance gradually decreased with increasing *tert*-butyl alcohol concentration from 0 to 350 mg/mL, which indicated that the peroxidase-like activity of β-$AgVO_3$ nanorods for catalytic oxidation of TMB in the presence of H_2O_2 originates from H_2O_2 decomposition to generate ·OH radicals.

Table 1. Elemental analysis of β-$AgVO_3$ nanorods by ICP-MS compared with the theoretical calculation

Methods	Ag element quality percentage (%)	V element quality percentage (%)
ICP-MS	53.93	22.88
Theoretical calculation	52.17	24.64

Optimization of experimental conditions

Similar to nanomaterial-based peroxidase mimetics and the natural enzyme (HRP), the catalytic activity of β-$AgVO_3$ nanorods was also dependent on the pH of the reaction buffer, incubation temperature, and H_2O_2 concentration. Therefore, various pH values (from 2.5 to 6.5), reaction temperatures (from 20 to 70°C), and H_2O_2 concentrations (from 0.1 to 1000 mM) were investigated. At the same time, the reaction pH, temperature, and H_2O_2 concentrations of HRP were also studied under the same conditions to compare their catalytic activity. The relative activity of β-$AgVO_3$ nanorods was higher in a weakly acidic (pH 4.0–5.0) solution than in a strongly acidic or neutral solution. Therefore, pH 4.0 was selected as the condition for subsequent experiments. With the

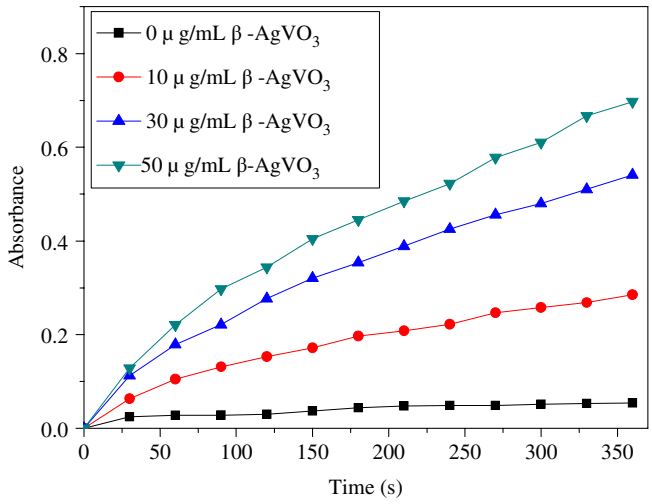

Fig. 4. Absorbance change at 652 nm versus time in the presence of 0 μg/mL (black), 10 μg/mL (red), 30 μg/mL (blue), and 50 μg/mL (green) β-$AgVO_3$ nanorods in the HAc–NaAc buffer (pH 4.0, 0.2 M) at room temperature.

temperature increasing from 20 to 70°C, the catalytic activity of β-$AgVO_3$ nanorods first increased and then decreased. Hence, room temperature (25°C) was taken as the optimum temperature. The optimal H_2O_2 concentration was found to be 8 mM. There values were very similar to those of HRP (Figure 6(a)–(c)). In addition, the effects of reaction time and concentration on the catalytic activity of β-$AgVO_3$ nanorods were also investigated. As shown in Figure 6(d), the relative activity of β-$AgVO_3$ nanorods gradually increased until reaction time up to 25 min, at which it reached a maximum. The catalytic activity of β-$AgVO_3$ nanorods gradually increased with increasing concentration of β-$AgVO_3$ nanorods. After the concentration reached 4.5 μg/mL, the relative activity changed very little (Figure 6(e)). Hence, 25 min of reaction time and 4.5 μg/mL of β-$AgVO_3$ nanorods were used for subsequent studies.

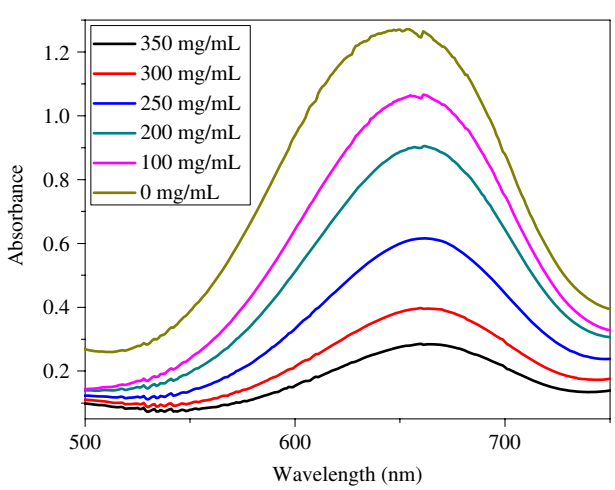

Fig. 5. Effect of different concentrations of *tert*-butyl alcohol on the oxidation of TMB.

Kinetic analysis of β-$AgVO_3$ nanorods as peroxidase mimics

The catalytic activity of β-$AgVO_3$ nanorods was investigated under the enzyme kinetics theory and methods using TMB and H_2O_2 as substrates under the optimal conditions (Figure 7(a) and (b)). HRP was also studied under the same conditions (Figure 7(c) and (d)). Typical Michaelis–Menten kinetic curves of the reactions were obtained by the changes of the respective substrate concentration in the catalytic system. The basic parameters could be calculated by using Lineweaver–Burk equation $1/v = (K_m/V_{max}) \times (1/[S]) + 1/V_{max}$ (v is the initial velocity, K_m is the Michaelis constant, V_{max} is the maximum reaction velocity, and [S] is the concentration of the substrate). The Michaelis–Menten constant (K_m) and the maximum initial velocity (V_{max}) of β-$AgVO_3$ nanorod peroxidase mimics and HRP are listed in Table 2. K_m is a measure of the enzyme affinity for a substrate. A smaller value of K_m indicates a stronger affinity between the enzyme and the substrate, and a more efficient catalysis. It could be seen that the K_m value of β-$AgVO_3$ nanorods with TMB as the substrate was lower than that of HRP and $AgVO_3$ nanobelts, which suggested that the β-$AgVO_3$ nanorods had higher affinity to TMB than HRP and $AgVO_3$ nanobelts.

Determination of glucose

Under the optimum conditions, a simple colorimetric determination method of glucose was developed combined with GO*x*. H_2O_2 could be produced by GO*x* catalytic oxidation of glucose solution; then ·OH generated by H_2O_2 decomposed. Finally, β-$AgVO_3$ nanorods could effect catalytic oxidation of TMB and produce a typical color reaction in the presence of H_2O_2. Based on this phenomenon, the changes of the absorbance at 652 nm with various concentrations of glucose were investigated. As shown in Figure 8(a), the color of the

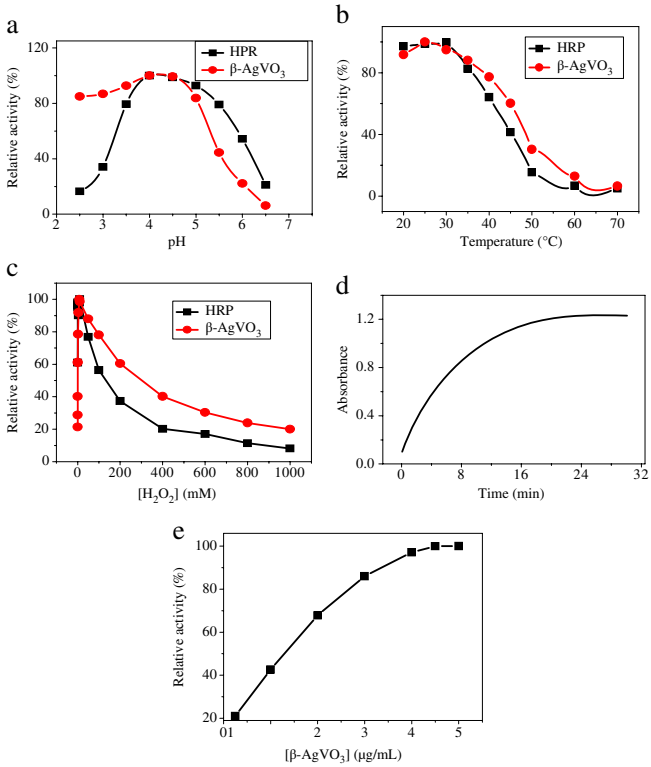

Fig. 6. Effect of pH (a), temperature (b), H_2O_2 concentration (c), reaction time (d), and β-$AgVO_3$ concentrations (e) on the catalytic reaction.

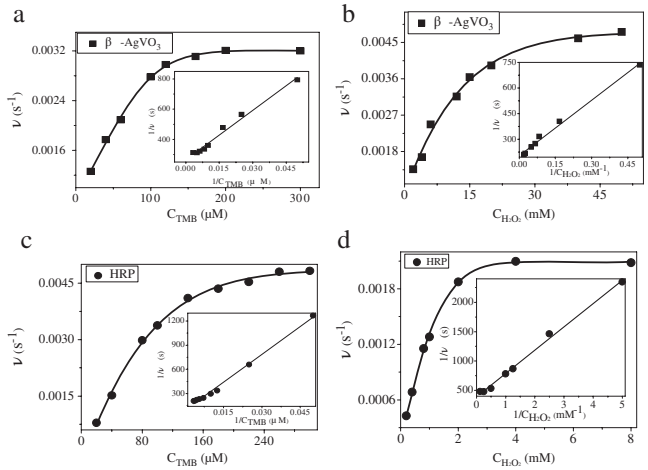

Fig. 7. Steady-state kinetic analyses using Michaelis–Menten model and Lineweaver–Burk model (insets) for β-$AgVO_3$ nanorods and by (a,c) varying the concentration of TMB with fixed H_2O_2 concentration and (b,d) varying the concentration of H_2O_2 with fixed TMB concentration.

solution changed deeper and deeper; at the same time, the absorbance at 652 nm increased gradually when the concentration of glucose ranged from 1.25 to 80 μM. A good linear relationship was found between the absorbance and the concentration of glucose from 1.25 to 60 μM (R^2 = 0.995) (Figure 8(b)), and the limit of detection of glucose was estimated to be 0.5 μM. When compared with other nanomaterial-based colorimetric sensors, the detection limit of the proposed colorimetric method is also comparable (Table 3). In addition, the proposed detection limit was evaluated by the formula $S/N = ((average_{sample} - average_{blank})/SD_{blank})$. And the sample concentration consistent with $3 < S/N < 5$ was defined as the limit of detection.[33]

Selectivity of the method

The selectivity for the detection of glucose was studied. The experiments, under the same conditions, were conducted to study the effects of the other foreign substances. As shown in Figure 9, these coexisting substances did not influence the detection of glucose and revealed the high selectivity of the β-$AgVO_3$ nanorods–TMB–H_2O_2 system for glucose detection. Thus, this system can be applied to glucose determination in real samples.

In order to verify the feasibility of the proposed colorimetric method, experiments using five human serum samples were conducted. The diluted serum sample solutions were detected under the same conditions as the standard for glucose determination. As can be seen, the results of the proposed colorimetric method

Table 2. Comparison the Michaelis–Menten constant (K_m) and the maximum reaction rate (V_{max}) of β-$AgVO_3$ nanorods with HRP and $AgVO_3$ nanobelts

Catalyst	Substance	K_m [mM]	V_{max} [10^{-4} s^{-1}]
β-$AgVO_3$ nanorods	TMB	0.04118	37.97
	H_2O_2	5.291	53.09
HRP	TMB	0.2422	104.01
	H_2O_2	1.018	25.65
$AgVO_3$ nanobelts[26]	TMB	8.03	—
	H_2O_2	14	—

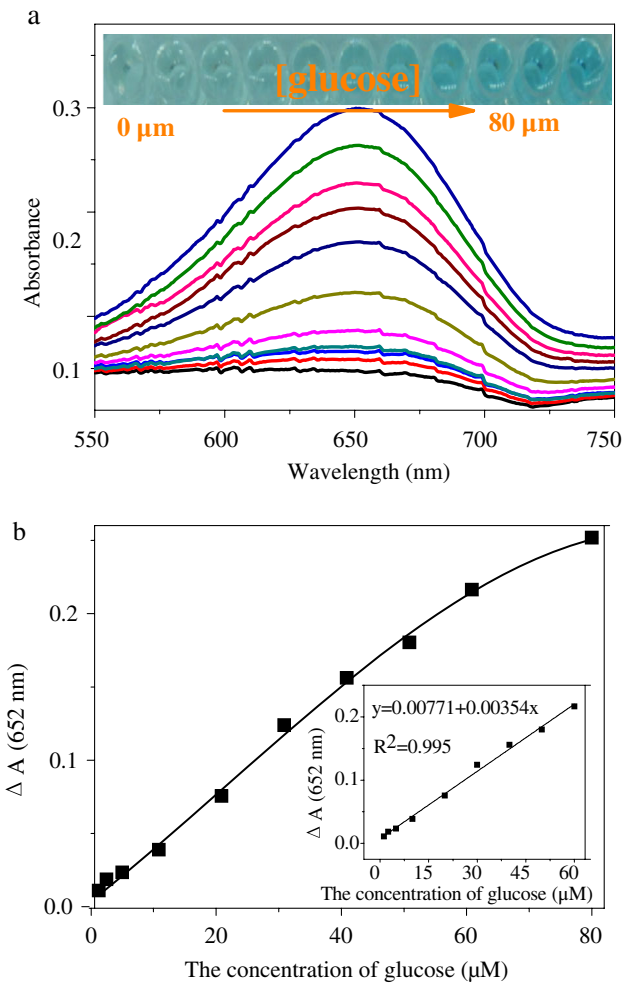

Fig. 8. (a) Effect of glucose on the absorption spectra in the GO*x*–β-$AgVO_3$ nanorods–TMB system. (b) Curve of glucose detection from 1.25 to 80 μM, where $\Delta A = A_{(glucose,652nm)} - A_{(blank,652nm)}$. Inset: (a) Color changes of the GO*x*–β-$AgVO_3$ nanorod–TMB system with different concentrations of glucose (from left to right: 0 to 80 μM), (b) Line calibration plot of the glucose determination.

were similar to those using the hospital's assay kit (Table 4). In addition, to demonstrate the reliability and precision of this colorimetric method further, the spiked recoveries of glucose in two serum samples were studied, and the results are listed in Table 5. The recovery values of these two serum samples range from 99.40 to 105.45%. These results show that the colorimetric method based on the peroxidase-like catalytic ability of β-$AgVO_3$ nanorods can applied to detect glucose in real samples.

Table 3. Comparison of various nanomaterial-based colorimetric sensing for glucose determination

Catalyst	Linear range (μM)	Detection limit (μM)	References
Ag nanoparticles	5–200	0.1	15
Ceria nanoparticles	6.6–130	3	29
Co_3O_4/rGO nanocomposites	1–100	1	30
$H_2TCPP - Fe_3O_4$	5–25	2.21	31
Pt–DNA complexes	0.1–1000	0.1	32
β-$AgVO_3$ nanorods	1.25–80	0.5	This work

CONCLUSION

In summary, β-$AgVO_3$ nanorods were shown to possess intrinsic peroxidase-like activity. The β-$AgVO_3$ nanorods could catalyze the oxidation of several substrates and generate a typical color reaction in the presence of H_2O_2. With O_2, GO*x* could catalyze the oxidation of glucose and then produce H_2O_2. The β-$AgVO_3$ nanorods had a higher affinity to TMB and a lower affinity to H_2O_2 compared to HRP. A simple, cheap, and selective colorimetric method was developed for glucose detection based on the above principles. In addition, this method was also tested in the detection of glucose in human serum samples. Furthermore, this

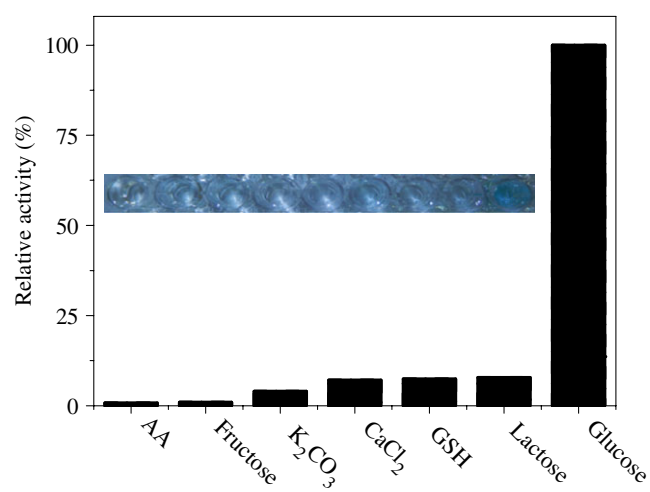

Fig. 9. Selectivity of the test using GO*x* and β-$AgVO_3$ nanorods for the determination of glucose. Insert: the corresponding color change of different samples. The concentrations of glucose and the other coexisting substances are 60 and 600 μM, respectively.

Table 4. Results of glucose detection in the real serum samples

Serum sample	Colorimetric method (mM, n = 3)	Glucose assay kit (mM)
1	13.16 ± 0.045	13.27
2	10.46 ± 0.040	11.15
3	8.74 ± 0.089	9.34
4	12.62 ± 0.078	13.30
5	8.36 ± 0.15	9.50

Table 5. Results for the determination of the glucose in two kinds of human serum sample

Original amount (μM)	Added (μM)	Found (μM)	Recovery (%)	RSD (%, n = 3)
13.16	5	18.35	103.80	1.41
	20	34.25	105.45	1.35
	40	54.80	104.10	0.46
10.46	5	15.43	99.40	0.39
	20	30.85	101.95	1.42
	40	52.06	104.00	2.03

method showed a good linear relationship, detection limit, and recovery value. Therefore, the proposed colorimetric method might open up new possibilities for the detection of glucose in complex systems.

ACKNOWLEDGMENTS

This work was supported by the Guangxi Natural Science Foundation of China (Nos. 2014GXNSFBA118045, 2014GXNSFBA118062 and 2015GXNSFAA139030), the scientific research project of Hechi University (No. XJ2015ZD004), and the scientific research project of the education department of Guangxi Zhuang Autonomous Region (Nos. YB2014331 and ZD2014113).

REFERENCES

1. H. Tan, C. Ma, L. Gao, Q. Li, Y. Song, F. Xu, T. Wang, L. Wang, *Chem. Eur. J.* **2014**, *20*, 1.
2. Y. Song, W. Wei, X. Qu, *Adv. Mater.* **2011**, *23*, 4215.
3. A. W. Martinez, S. T. Phillips, M. J. Butte, G. M. Whitesides, *Angew. Chem. Int. Ed.* **2007**, *46*, 1318.
4. H. Wei, E. Wang, *Chem. Soc. Rev.* **2013**, *42*, 6060.
5. J. Li, J. Du, J. Zhang, *J. Chin. Chem. Soc.* **2014**, *61*, 1395.
6. Y. Kim, R. C. Johnson, J. T. Hupp, *Nano Lett.* **2001**, *1*, 165.
7. W. Liu, H. Yang, Y. Ding, S. Ge, J. Yu, M. Yan, X. Song, *Analyst* **2014**, *139*, 251.
8. L. Z. Gao, J. Zhuang, L. Nie, J. B. Zhang, Y. Zhang, N. Gu, T. H. Wang, J. Feng, D. L. Yang, S. Perrett, X. Y. Yan, *Nat. Nanotechnol.* **2007**, *2*, 577.
9. A. Asati, S. Santra, C. Kaittanis, S. Nath, J. M. Perez, *Chem. Int. Ed.* **2009**, *48*, 2308.
10. J. Yin, H. Cao, Y. Lu, *J. Mater. Chem.* **2012**, *22*, 527.
11. R. André, F. Natálio, M. Humanes, J. Leppin, K. Heinze, R. Wever, H.-C. Schröder, W. E. G. Müller, W. Tremel, *Adv. Funct. Mater.* **2011**, *21*, 501.
12. W. Chen, J. Chen, A.-L. Liu, L.-M. Wang, G.-W. Li, X.-H. Lin, *ChemCatChem* **2011**, *3*, 1151.
13. Y. Wan, P. Qi, D. Zhang, J. Wu, Y. Wang, *Biosens. Bioelectron.* **2012**, *33*, 69.
14. Y. J. Long, Y. F. Li, Y. Liu, J. J. Zheng, J. Tang, C. Z. Huang, *Chem. Commun.* **2011**, *47*, 11939.
15. H. Jiang, Z. Chen, H. Cao, Y. Huang, *Analyst* **2012**, *137*, 5560.
16. L. Chen, N. Wang, X. Wang, S. Ai, *Microchim. Acta* **2013**, *180*, 1517.
17. W. Zhang, X. Liu, D. Walsh, S. Yao, Y. Kou, D. Ma, *Small* **2012**, *8*, 2948.
18. X. Hu, A. Saran, S. Hou, T. Wen, Y. Ji, W. Liu, H. Zhang, W. He, J.-J. Yin, X. Wu, *RSC Adv.* **2013**, *3*, 6095.
19. Y. Song, K. Qu, C. Zhao, J. Ren, X. Qu, *Adv. Mater.* **2010**, *22*, 2206.
20. Y. Song, X. Wang, C. Zhao, K. Qu, J. Ren, X. Qu, *Chem. Eur. J.* **2010**, *16*, 3617.
21. W. Shi, Q. Wang, Y. Long, Z. Cheng, S. Chen, H. Zheng, Y. Huang, *Chem. Commun.* **2011**, *47*, 6695.
22. L. Su, J. Feng, X. Zhou, C. Ren, H. Li, X. Chen, *Anal. Chem.* **2012**, *84*, 5753.
23. K. Zhang, W. Zuo, Z. Wang, J. Liu, T. Li, B. Wang, Z. Yang, *RSC Adv.* **2015**, *5*, 10632.
24. T. Tian, L. Ai, X. Liu, L. Li, J. Li, J. Jiang, *Ind. Eng. Chem. Res.* **2015**, *54*, 1171.
25. L. Su, W. Qin, H. Zhang, Z. U. Rahman, C. Ren, S. Ma, X. Chen, *Biosens. Bioelectron.* **2015**, *63*, 384.
26. Z. Xiang, Y. Wang, P. Ju, D. Zhang, *Microchim. Acta* **2016**, *183*, 457.
27. A. Y. S. Malkhasian, *J. Alloys Compd.* **2015**, *649*, 394.
28. G. V. Buxton, C. L. Greenstock, W. P. Heiman, A. B. Ross, *J. Phys. Chem. Ref. Data* **1988**, *17*, 513.
29. X. Jiao, H. Song, H. Zhao, W. Bai, L. Zhang, Y. Lv, *Anal. Methods* **2012**, *4*, 3261.

30. J. Xie, H. Cao, H. Jiang, Y. Chen, W. Shi, H. Zheng, Y. Huang, *Anal. Chim. Acta* **2013**, *796*, 92.
31. Q. Liu, H. Li, Q. Zhao, R. Zhu, Y. Yang, Q. Jia, B. Bian, L. Zhuo, *Mater. Sci. Eng. C* **2014**, *41*, 142.
32. X. Chen, X. Zhou, J. Hu, *Anal. Methods* **2012**, *4*, 2183.
33. L. Guo, Y. Xu, A. R. Ferhan, G. Chen, D.-H. Kim, *J. Am. Chem. Soc.* **2013**, *135*, 12338.

